ATP-Dependent Paracrine Intercellular Communication in Cultured Bovine Corneal Endothelial Cells

Priya Gomes,[1] *Sangly P. Srinivas,*[2] *Johan Vereecke,*[1] *and Bernard Himpens*[1]

Purpose. Intercellular communication (IC) in nonexcitable cells is mediated through gap junctions and/or through the release of paracrine mediators. This study was conducted to investigate adenosine-5′ triphosphate (ATP)-dependent paracrine IC in the propagation of Ca^{2+} waves in confluent monolayers of cultured bovine corneal endothelial cells (BCECs).

Methods. A Ca^{2+} wave was induced by point mechanical stimulation (PMS) of a single cell by indentation with a glass micropipette (~1 μm tip) for <1 second. Dynamic changes in $[Ca^{2+}]_i$ in the mechanically stimulated (MS) cell and in the neighboring (NB) cells were visualized with a confocal microscope, using a fluorescent dye. Normalized fluorescence (NF), calculated as the ratio of the average fluorescence of a cell to the average under resting conditions, was used as a measure of $[Ca^{2+}]_i$. Expression of P2Y receptors and ecto-adenosine triphosphatases (ATPases) was investigated by RT-PCR. ATP release in response to PMS was measured by luciferin-luciferase (LL) bioluminescence.

Results. BCECs subjected to PMS showed a transient $[Ca^{2+}]_i$ increase. Under control conditions, the maximum NF in the MS cell occurred within 600 ms, and the fluorescence returned to baseline within 170 seconds. NB cells also presented a $[Ca^{2+}]_i$ increase with a transient characterized by decreasing maximum NF and increasing latency as a function of the distance from the MS cell. These transients propagated as an intercellular Ca^{2+} wave to a distance of five or six NB cells away from the MS cell, covering areas (called active areas, AAs) up to 77,000 ± 3,200 μm^2 ($N = 21$). The percentage of responsive cells (defined as cells showing maximum NF > 1.1) decreased with increasing distance from the MS cell. The Ca^{2+} wave crossed cell-free lanes. Pretreatment of cells with the nonselective purinergic receptor antagonist suramin (200 μM), exogenous apyrases, which break down nucleotides (10 U/mL), or the PLC inhibitor U-73122 (10 μM) reduced the wave propagation, whereas the ecto-ATPase inhibitor ARL-67156 (100 μM) significantly enhanced it. ATP-dependent LL bioluminescence increased after PMS. RT-PCR showed mRNAs for P2Y1 and P2Y2 receptors and ecto-ATPases in BCECs.

Conclusions. PMS of BCECs induces release of ATP and a concomitant intercellular Ca^{2+} wave, even in the absence of direct cell–cell contacts. The AA of the wave is modulated by agents that affect P2Y receptor activity. Thus, PMS-induced intercellular Ca^{2+} wave propagation in BCECs involves ATP-dependent paracrine IC. (*Invest Ophthalmol Vis Sci.* 2005;46:104–113) DOI:10.1167/iovs.04-0846

The corneal endothelium plays an important role in corneal transparency, which depends on the hydration state of the stroma.[1] The cells of this monolayer act as gatekeepers for entry of solutes and water into the stroma, and at the same time they pump fluid from the stroma into the anterior chamber.[2–4] Even though recent findings suggest a role of the corneal epithelium in fluid transport,[5] it is the endothelial fluid transport that largely counterbalances the fluid leak into the stroma, leading to constant stromal hydration.[2]

Several investigations to date have unraveled G-protein–coupled receptors that are likely to influence the barrier integrity and pump functions of the corneal endothelium.[6–14] Specifically, recent studies have focused on the function of purinergic P1 and P2 receptors in the endothelium.[6,9–11,14] In rabbit corneal endothelial cells, adenosine has been shown to activate the A2B subtype of P1 receptors, leading to stimulation of fluid transport and enhancement of barrier integrity.[10,11] Adenosine-5′ triphosphate (ATP), in contrast, has been shown to stimulate P2Y receptors, leading to activation of Cl^- channels,[9] enhancement of regulatory volume decrease,[14] and increase in cell proliferation.[15] In other cell types, ATP is known to be pleiotropic, with significant effects on ion channels, apoptosis, and barrier integrity.[16–24] It has also been shown that ATP forms a paracrine mediator of intercellular communication (IC) in many cell types, including glial cells, epithelium, and vascular endothelium.[25–31]

In most tissues of the body, IC is essential for coordinated cellular activity to maintain tissue homeostasis. As in excitable cells, many nonexcitable cells are also capable of IC through two pathways: gap junctional intercellular communication (GJIC) and paracrine intercellular communication (PIC). In GJIC, second messengers and metabolites are exchanged through gap junctions formed by the docking of two hemichannels contributed by two adjacent cells.[32] In contrast with GJIC, PIC involves release of one or more diffusible extracellular signaling molecules, enabling paracrine effects. A widely investigated paracrine mediator is the endogenous P2 agonist ATP. Several intra- and extracellular stimuli release ATP, which then activates P2 receptors on the neighboring cells and thereby elicits a coordinated multicellular response. In the case of a Ca^{2+} transient evoked by mechanical stimulation, intercellular propagation of the Ca^{2+} wave is elicited by means of ATP release followed by diffusion of the messenger to neighboring cells and activation of their P2 receptors.

Although insight has been gained in the recent past about PIC and GJIC, their importance in a given cell type or their engagement in response to a specific extracellular stress remains poorly understood. In the context of the corneal endothelium, the significance of IC to tissue homeostasis is not evident, although it is well known that point injuries and defects of the monolayer occur, resulting in heterogeneity. IC may be involved in the restoration of the integrity of the endothelial layer. The fact that corneal endothelial cells are

From the [1]Laboratory of Physiology, KULeuven, Campus Gasthuisberg, Leuven, Belgium; and the [2]Indiana University, School of Optometry, Bloomington, Indiana.

Supported by National Eye Institute Grants EY11107 and EY14415 (SPS); FWO-Vlaanderen Grants G.0218.03 and GOA/2004/07; IAP program 5/05 (BH, JV); and IRO KULeuven (PG).

Submitted for publication July 20, 2004; revised September 13, 2004; accepted September 16, 2004.

Disclosure: **P. Gomes**, None; **S.P. Srinivas**, None; **J. Vereecke**, None; **B. Himpens**, None

The publication costs of this article were defrayed in part by page charge payment. This article must therefore be marked "*advertisement*" in accordance with 18 U.S.C. §1734 solely to indicate this fact.

Corresponding author: Johan Vereecke, Laboratory of Physiology, KULeuven, Campus Gasthuisberg O/N, B-3000 Leuven, Belgium; johan.vereecke@med.kuleuven.ac.be.

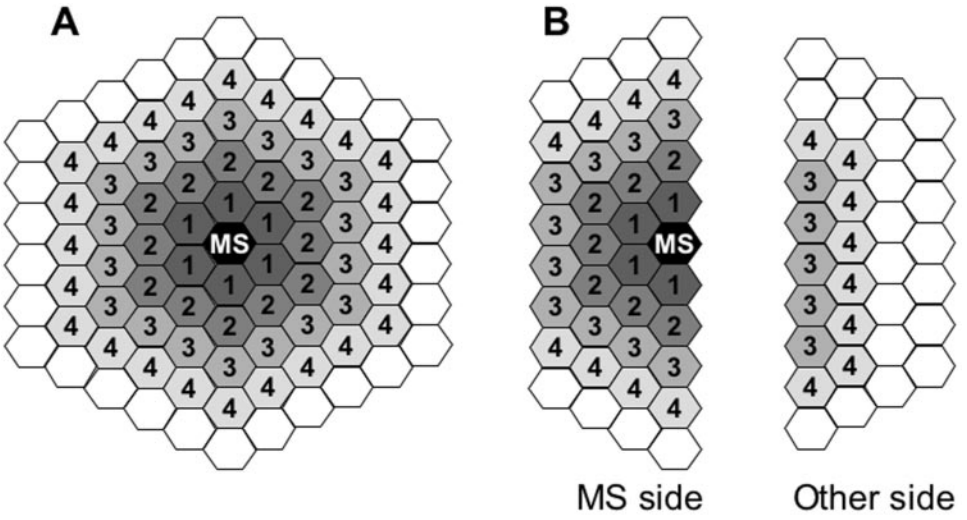

FIGURE 1. Definition of neighboring (NB) cell layers. (**A**) A confluent monolayer. Hexagon labels: MS, the mechanically stimulated cell; 1, in direct contact with the MS cell, representing neighboring cell layer NB1; 2 and 3, cell layers NB2 and NB3. (**B**) A monolayer with a cell-free lane that was obtained by scratching off cells with a needle. MS side, the side where the MS cell is located; other side, side across the cell-free lane. The cell-free lanes were 30 to 110 μm wide.

nonproliferative suggests that the monolayer becomes senescent with reduced functional capacity vis-à-vis aging. Because cellular senescence is known to influence the expression density of certain connexins,[33–36] it is likely that aged endothelial cells have reduced GJIC. This adds further impetus to examine PIC in the corneal endothelium.

The major objective of this study was to examine the role of PIC in the intercellular Ca^{2+} wave propagation in corneal endothelial cells. Using point mechanical stimulation (PMS) in bovine corneal endothelial cells (BCECs), this study showed intercellular Ca^{2+} wave propagation mediated by PIC involving P2Y receptors. Accordingly, both the intensity and distance of the propagation were reduced significantly by the activity of ectonucleotidases and P2Y antagonists.

MATERIALS AND METHODS

Cell Culture

Primary cultures of BCECs were established as previously described.[14,37] The growth medium contained Dulbecco's modified Eagle's medium (cat no: 11960-044; Invitrogen-Gibco, Karlsruhe, Germany) supplemented with 10% fetal bovine serum (cat no. F7524; Sigma-Aldrich, Deisenhofen, Germany), 6.6% Glutamax (cat no. 35050-038; Invitrogen-Gibco), and 1% antibiotic-antimycotic mixture (cat no. 15240-096; Invitrogen-Gibco). Cells were grown at 37°C in a humidified atmosphere containing 5% CO_2. Cells of the second and third passages were harvested and seeded into two chambered glass slides (Laboratory-Tek, cat no: 155380; Nunc, Rosklide, Denmark) at a density of 165,000 cells per chamber (4.2 cm^2), unless otherwise stated. Cells were allowed to grow to confluence for 3 or 4 days before use. Tightly packed cells of uniform size form highly ordered confluent monolayers that closely resemble the arrangement of native corneal endothelium.[38] The cells undergo terminal differentiation, show characteristic polygonal morphology,[38] and do not possess a fibroblast-like appearance. The fresh or cultured cells were shown to possess several exchangers, cotransporters, and channels that participate in corneal endothelial fluid transport.[39,40] Fresh or cultured BCECs possess polarized ion transport proteins[41–43] that mediate basolateral-to-apical fluid transport.[2]

Measurement of $[Ca^{2+}]_i$

Cells were loaded with a Ca^{2+}-sensitive dye (10 μM; Fluo-4 AM; Molecular Probes, Eugene, OR) for 30 minutes at 37°C. The dye was excited at 488 nm, and the resultant fluorescence emission was collected at 530 nm. Spatial changes in $[Ca^{2+}]_i$ after PMS were measured on a laser scanning fluorescence microscope (model LSM510; Carl Zeiss Meditec, Jena, Germany) using a 40× objective, unless otherwise stated. Images were collected and stored on a computer. Polygonal regions of interest (ROIs) were drawn to define the borders of each cell (Fig. 1A). The central cell, labeled MS, was the mechanically stimulated cell. The neighboring (NB) cells immediately surrounding the MS cell were defined as neighboring cell layer 1 (NB1), the ones immediately surrounding the NB1 cells were defined as neighboring cell layer 2 (NB2), and so on. Fluorescence was averaged over the area of each ROI. Normalized fluorescence (NF) was then obtained by dividing the fluorescence by the average fluorescence before PMS. Intercellular Ca^{2+} wave propagation was characterized by maximum NF, delay, and percentage of responsive cells (%RCs), as well as the total surface area of responsive cells (active area, AA) with NF $\geq$ 1.1.

Reverse Transcription–Polymerase Chain Reaction

Total RNA was extracted from confluent cells grown on T25 flasks with an extraction kit (RNeasy; Qiagen, Valencia, CA). First-strand cDNA synthesis was then performed (Advantage RT-for-PCR Kit; BD-Clon-

TABLE 1. Primers Used for RT-PCR Amplification of P2Y1, P2Y2, CD39, and CD73

Gene	Accession No.	Primer	Sequence (5′ to 3′)	Tm (°C)	Homology	Size (bp)
P2Y1	X87628	Forward	TCCCTAGGGAAAGCGCAGTC	64	Bovine	561
		Reverse	GAACATCCAGATGGCCACGC	64		
P2Y2	AF005153	Forward	CCCCTGTGCTGTACTTCGTCAC	68	Bovine	274
		Reverse	GCAGAGGACGAAGACAGTCAGC	70		
CD39	AF005940	Forward	GAAGGTGCCTATGGCTGGATTAC	55	Human/rat/mouse	870
		Reverse	TGTTGGTCAGGTTCAGCATGTAG	55		
CD73	AF034840	Forward	AGTACCAGGGCACCATCTGGTTC	55	Human/rat/mouse	1317
		Reverse	ATATCTTGGTCACCAGAGTCATG	55		

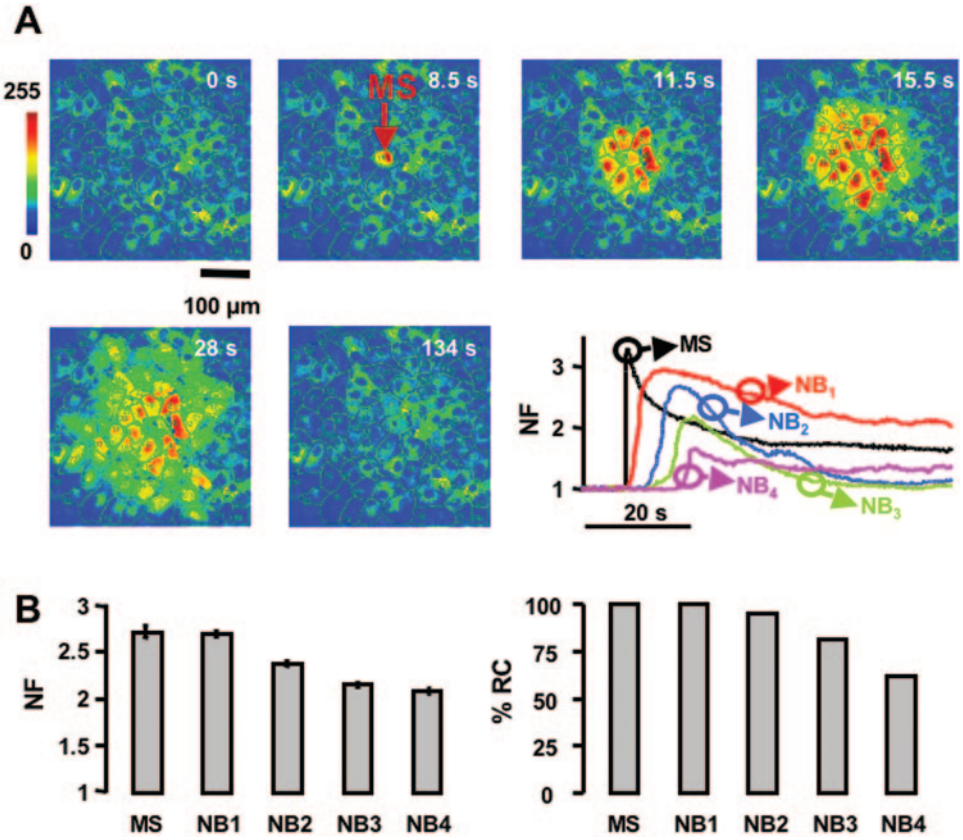

FIGURE 2. Intercellular Ca^{2+} wave propagation elicited by mechanical stimulation. Cells were loaded with a fluorescent dye (Fluo-4 AM; Molecular Probes, Eugene, OR) and a single cell (MS cell) was subjected to PMS. (**A**) Pseudocolored fluorescence images at different time points after mechanical stimulation. The color scale at the *top left* represents the fluorescence changes induced by the $[Ca^{2+}]_i$ changes. The first image shows the fluorescence intensities before stimulation. The *red arrow* in the second image (time = 8.5 seconds) identifies the MS cell. The time course of $[Ca^{2+}]_i$-sensitive fluorescence of MS and a typical cell from different NB layers is shown as a line graph at the *top right* of each panel. Note the delay in the onset of the Ca^{2+} increase in NB cell layers. (**B**) *Left*: the maximum NF in the MS cell and in responsive NB cells. The number of cells for MS and NB1 to NB4 was 125, 851, 1546, 1767, and 1256, respectively. The number of MS cells corresponds to the number of independent experiments. *Right*: the %RC for each of the NB cell layers.

tech, Palo Alto, CA). PCR was performed with the following parameters: (1) initial denaturation at 95°C for 4 minutes, (2) denaturation at 95°C for an additional minute, (3) annealing at 56°C to 58°C for 1 minute, and (4) extension at 72°C for 2 minutes. Steps 2 through 4 were repeated for ~35 cycles. The final extension step lasted for 10 minutes, and the final products were cooled to 4°C for ~10 minutes. Negative control experiments were performed in the absence of reverse transcriptase during the RT reaction. All PCR products, along with DNA ladders (Invitrogen-Gibco), were visualized on a 1% ethidium bromide–stained agarose gel and illuminated with UV light. The PCR products were confirmed by DNA sequencing. Table 1 is a list of the primers used for detecting P2Y receptors and ectonucleotidases.

ATP Measurements

The accumulation of released ATP in a solution bathing a monolayer of BCECs was probed with the luciferin-luciferase (LL) bioluminescence assay. Photons emitted as a result of the oxidation of luciferin by luciferase in the presence of ATP and O_2 were detected by a photon-counting photomultiplier tube (H7360-01; Hamamatsu, Hamamatsu City, Japan), with a sensitive area 25 mm in diameter and positioned 20 mm above the cells. Voltage pulses from the photomultiplier module were counted with a high-speed counter (PCI-6602; National Instruments Co., Austin, TX). The dark count of the photomultiplier tube was <80 counts/s.

Mechanical Stimulation

The PMS of a single BCEC consisted of a short-lasting deformation of the cell by briefly touching <1% of the cell membrane with a glass micropipette (tip diameter <1 μm) coupled to a piezoelectric nanopositioner (P-280 piezo stage operated through an E463 amplifier/controller; PI Polytech, Karlsruhe, Germany) mounted on a micromanipulator.

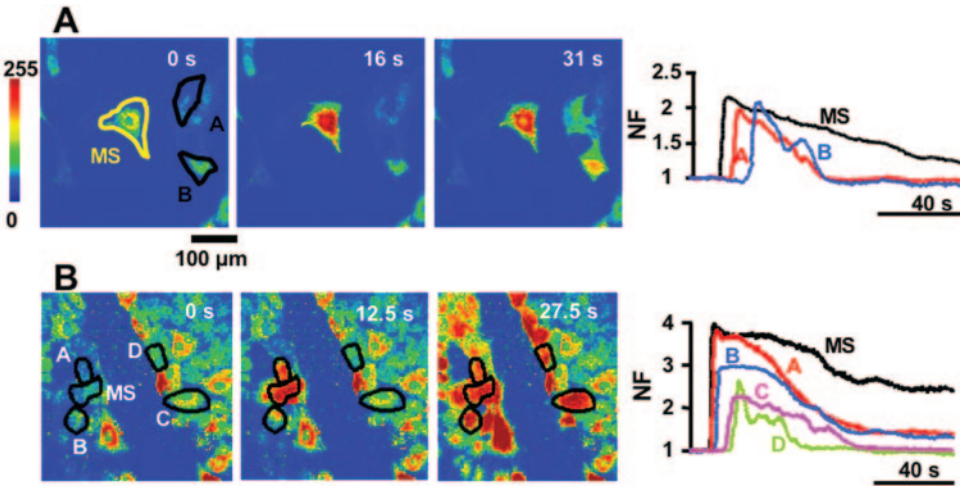

FIGURE 3. Ca^{2+} wave propagation in unconnected cells. (**A**) Fluorescence images of Ca^{2+} wave propagation in sparsely seeded cells (*left*) and graphs representing the time course of NF in MS and two NB cells (*right*). Note that both cells A and B are disconnected from the MS cell. (**B**) Ca^{2+} wave propagation in confluent cells with cell-free lanes (*left*) and graphs representing the time course of NF in MS and 4 different cells labeled A–D in the first image (*right*). Cells A and B are connected to the MS cell. Cells C and D are at the other side of the cell-free lane.

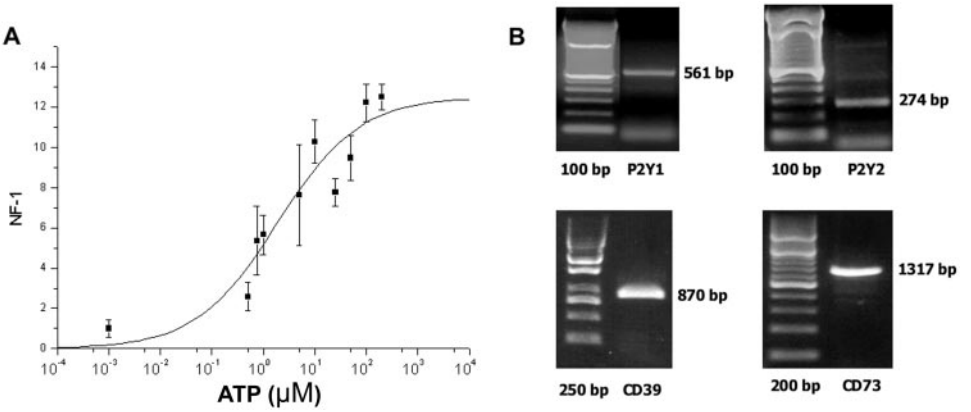

FIGURE 4. P2Y receptors and ectonucleotidases in BCECs. (**A**) Dose–response curve for the effect of ATP on intracellular Ca^{2+} (expressed in terms of NF) in BCECs. EC_{50} = 1.47 μM. Hill coefficient = 0.53. Each point on the curve is the average of at least five experiments. (**B**) RT-PCR identification of P2Y1, P2Y2, CD39, and CD73 in total RNA extracted from BCECs.

Chemicals

6-Carboxyfluorescein diacetate (cat no. C1362) was obtained from Molecular Probes. PBS (cat no. 14190-094) was obtained from Invitrogen-Gibco. Suramin (cat no. S2671), apyrase VI (cat no. A6410), apyrase VII (cat no. A6535), ARL-67156 (6-*N*,*N*-diethyl-β,γ-dibromomethylene-D-ATP, cat no: A265), U-73122 (cat no. U6756), U-73343 (cat no. U6881), ATP assay mix (cat name: FLAAM), and ATP were obtained from Sigma-Aldrich.

Data Analysis

All data are given as the mean ± SEM. Comparisons of means between groups were performed by unpaired t-tests, with $P < 0.05$ considered a statistically significant difference. *N* indicates the number of independent experiments (the number of cells subjected to PMS) while *n* represents the total number of cells.

RESULTS

Intercellular Ca^{2+} Wave Evoked by PMS

In the first series of experiments, we assessed the characteristic parameters of the Ca^{2+} wave induced by mechanical stimulation. In response to PMS, the MS cell showed an initial increase in Ca^{2+} that originated at the point of stimulation and spread throughout the MS cell. On reaching the boundaries of the MS cell, the Ca^{2+} increase was found to spread out to the NB cells in a wave-like manner, as shown by fluorescence images in Figure 2A. The NF in the MS cell was higher than in the NB cells, and the NF in the NB cells decreased with increasing distance from the MS cell. In control conditions, Ca^{2+} transients were observed up to approximately four to six cell layers away from the MS cell. The time course of the Ca^{2+} transients (i.e., NF versus t) in representative cells of the images is shown in the line plot in Figure 2A. Note that the decrease in maximum NF, as well as an increase in the time delay of the NB cells with increasing distance from the MS cell, is clearly evident. Figure 2B summarizes results from all experiments. A maximum NF of 2.7 ± 0.06 (N = 125) was obtained in the MS cell. After the peak, which was reached in approximately 4.1 ± 0.2 seconds. The NF in the MS cell showed a very gradual and slow decline, returning to the basal value after 171 ± 4 seconds after application of the stimulus.

The maximum NFs in NB1, -2, -3, and -4 (representing NB cell layers 1, 2, 3, and 4) were 2.7 ± 0.03 (n = 849), 2.4 ± 0.02 (n = 1469), 2.2 ± 0.02 (n = 1430), and 2.1 ± 0.03 (n = 778), respectively (Fig. 2B, left). The delay in response to PMS also increased with increasing distance of the NB layer from the MS cell. The response of the NB cells showed a delay of 1.8 ± 0.06, 4.8 ± 0.07, 7.5 ± 0.1, and 9.7 ± 0.2 seconds (for NB1, -2, -3, and -4, respectively). The %RC for MS was 100%. %RC for NB1, -2, -3, and -4 cells was 100%, 95%, 81%, and 62%, respectively, thus also decreasing as a function of the cell layer away from the MS cell (Fig. 2B, right). The average AA was 77,000 ± 3,200 μm^2 (N = 21) in control conditions. These data, demonstrate the presence of a decremental, centrifugally propagating intercellular Ca^{2+} wave in BCECs in response to PMS.

PIC in Cells without Cell–Cell Contacts

To find out whether PIC contributes to the wave propagation, we examined wave propagation in the absence of cell–cell contacts. This was achieved by sparse seeding of cells (Fig. 3A) or by deliberate scratching of confluent monolayers (Fig. 3B) to yield cell-free lanes (Fig. 1B) with a width of 30 to 110 μm (average = 54 μm, N = 15). In both of these conditions, the Ca^{2+} wave was found to jump over the gaps between MS and NB cells, demonstrating that an extracellular messenger, released by the MS cell, contributes to the propagation of the Ca^{2+} wave upon PMS.

P2Y Receptors in BCEC

ATP is the prime candidate for mediating paracrine IC in the Ca^{2+} wave propagation through its extracellular action on the P2 family of purinergic receptors. We determined the dose–response curve of the NF of BCECs in response to exogenous ATP. As shown in Figure 4A, the EC_{50} for ATP in BCECs is 1.5 μM, with a saturating NF response noted at approximately 100 μM. Consistent with the response to ATP in our experiments and with the functional characterization by Srinivas et al.,[14] we also found expression of P2Y receptors and ecto-ATPases at the mRNA level. Figure 4B shows expression of P2Y1, P2Y2, CD39, and CD73 in BCECs by RT-PCR. P2Y1 and P2Y2 are GPCRs sensitive to endogenous ATP, whereas CD39 and CD73 are ectonucleotidases known to metabolize ATP to adenosine monophosphate (AMP) by CD39, and subsequently AMP to adenosine by CD73.

PMS Induced Release of ATP

To study whether BCECs release ATP, we measured basal extracellular ATP levels by the LL technique. In control conditions, we found a small basal release of ATP that increased markedly on PMS in 10 of 10 experiments. These experiments demonstrate that ATP is available to act as an extracellular messenger for the wave propagation upon PMS.

Effect of Inhibitors of Purinergic Activity on Ca^{2+} Wave Propagation

Next, we investigated whether the modulation of P2Y transmission affects IC in BCECs. In the first set of experiments, we studied the effect of blocking P2Y receptors, by using the

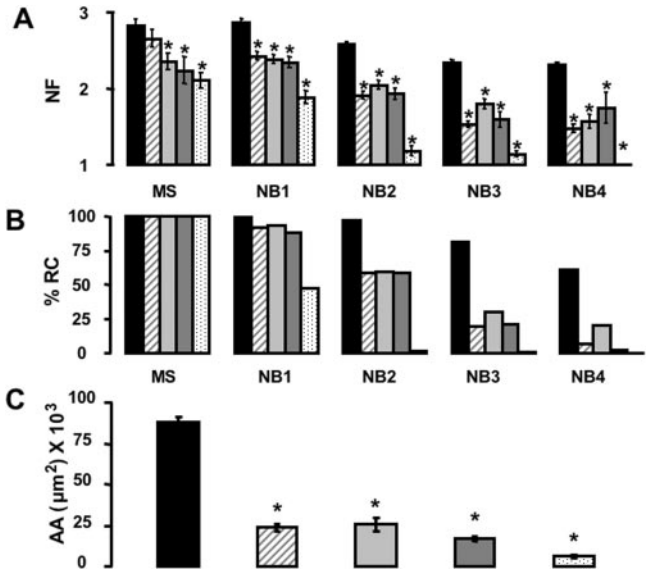

FIGURE 5. Reduced Ca^{2+} wave propagation in the presence of purinergic modulators. Cells were treated with suramin (200 μM), apyrase VI (10 U/mL), apyrase VII (10 U/mL), or apyrase VI+VII (5 U/mL each) for 30 minutes. The Ca^{2+} wave propagation in response to PMS is represented in control (*black bars*; $N = 53$), suramin (*hatched bars*; $N = 42$), apyrase VI (*light gray bars; N* = 25), apyrase VII (*dark gray bars*; $N = 17$), and apyrase VI+VII (*dotted bars*; $N = 21$). *$P < 0.05$ versus control.

nonselective P2Y receptor antagonist suramin. In the presence of 200 μM suramin,[27,44] neither the NF (Fig. 5A) nor the %RC (Fig. 5B) of the MS cells ($N = 42$) was significantly different from control condition ($N = 53$; Table 2). However, the %RC of NB cells was reduced markedly from NB2 onward when compared with the controls (NB1: 92% vs. 99%, NB2: 59% vs. 97%, NB3: 19% vs. 81%, NB4: 6% vs. 61%; Fig. 5B). Consequently, AA was reduced (Fig. 5C, Table 2).

We also studied the effect of nucleotide hydrolysis by exogenous apyrase VI (which has a high ATPase/adenosine diphosphatase [ADPase] ratio) or apyrase VII (which preferentially hydrolyzes adenosine diphosphate [ADP]).[27] Similar to the effect of suramin, the presence of apyrase VI (10 U/mL; $N = 25$) or apyrase VII (10 U/mL; $N = 17$) resulted in an inhibition of the Ca^{2+} wave propagation (Fig. 5, Table 2). Apyrase VII caused a somewhat stronger inhibition in the outermost cell layers when compared to apyrase VI. The combination of 5 U/mL apyrase VI and 5 U/mL apyrase VII had a cumulative effect, causing a more pronounced inhibition of the Ca^{2+} wave than either 10 U/mL apyrase VI or 10 U/mL apyrase VII (Fig. 5, Table 2), limiting the propagation to NB1. These experiments demonstrated that PIC, via an agonist of P2Y receptors, is involved in the IC upon PMS and provide evidence that both ATP and ADP are involved.

Ca^{2+} Wave Propagation in the Presence of Inhibitors of Ectonucleotidase Activity

We next investigated the effect of inhibiting endogenous ectonucleotidase activity by application of 100 μM ARL-67156.[45] Using a 10× objective, we saw that the presence of ARL-67156 caused a threefold increase of AA of cells reached by the Ca^{2+} wave when compared to control conditions (840,000 ± 110,000 μm^2; $N = 6$, vs. 210,000 ± 25,000 μm^2; $N = 4$; Fig. 6). In addition to a larger AA, the propagation of the wave is faster and more intense, as seen in the line plots of Figure 6. This is the result of higher concentrations of the nucleotides in the extracellular spaces surrounding NB cells in the presence of ARL-67156. These experiments demonstrated that PIC, via a purinergic mediator, is involved in the Ca^{2+} wave propagation

TABLE 2. Average Maximum NF, Percentage of Responsive Cells, and Average AA in MS and NB Cells

	MS	NB1	NB2	NB3	NB4	Active Area (AA, μm^2)
Control						
NF	2.8	2.9	2.6	2.3	2.3	
SEM	0.09	0.04	0.03	0.03	0.04	
n	53	367	650	750	578	
%RC	100	99	97	81	61	87,521 ± 3,110
Suramin (200 μM)						
NF	2.7	2.4*	1.9*	1.5*	1.5*	
SEM	0.11	0.05	0.05	0.04	0.06	
n	42	292	462	598	468	
%RC	100	92	59	19	6	23,303 ± 1,865*
Apyrase VI (10 U/mL)						
NF	2.4*	2.4*	2.0*	1.8*	1.6*	
SEM	0.11	0.06	0.06	0.06	0.09	
n	25	163	233	254	159	
%RC	100	93	60	30	20	25,659 ± 4,012*
Apyrase VII (10 U/mL)						
NF	2.2*	2.3*	1.9*	1.6*	1.7*	
SEM	0.20	0.10	0.10	0.10	0.20	16,903 ± 1,886*
n	17	119	164	173	124	
%RC	100	88	59	21	2	
Apyrase VI + VII (5 U/mL each)						
NF	2.1*	1.9*	1.2*	1.1*	1.1*	
SEM	0.10	0.09	0.06	0.03	0.02	5,922 ± 850*
n	21	130	262	287	196	
%RC	100	47	2	1	0	

Data were collected during mechanical stimulation in control conditions and in cells treated with suramin (200 μM), apyrase VI (10 U/mL), apyrase VII (10 U/mL), or apyrase VI + VII (5 U/mL each).
* $P < 0.05$ versus control.

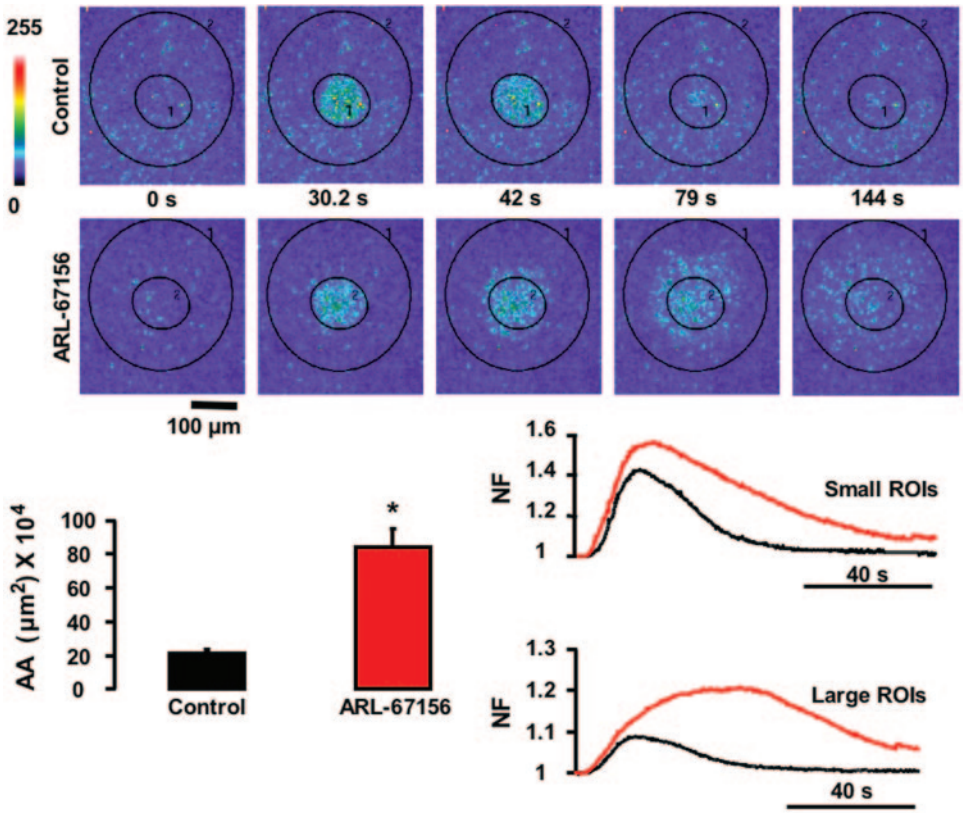

FIGURE 6. Enhanced Ca^{2+} wave propagation in the presence of an ecto-ATPase inhibitor. Ca^{2+} wave propagation was characterized in response to PMS using the 10× instead of the 40× objective. The fluorescence images represent the time course of the Ca^{2+} wave in control conditions (*top*) and after pretreatment with 100 μM ARL-67156 for 30 minutes. Two polygons were drawn on both time series of Ca^{2+} waves, respectively representing the AA observed under control conditions (small ROI) and in the presence of ARL-67156 (large ROI). *Bottom left*: AA in both conditions; *bottom right*: the normalized fluorescence averaged over the small and the large ROIs as a function of time. *Black lines*: Ca^{2+} increase in control conditions; *red lines:* Ca^{2+} increase after pretreatment with ARL-67156. Note that the average Ca^{2+} increase is higher and the propagation is faster and more prolonged in time in the presence of ARL-67156.

upon PMS and provide evidence that both ATP and ADP are involved.

Effect of Modulators of Purinergic Activity on the Ca^{2+} Wave across Cell-Free Lanes

The Ca^{2+} wave propagation across cell-free lanes was largely or completely blocked on pretreatment of the cells with suramin (Fig. 7A, top row) or apyrases (Fig. 7A, middle row), whereas it was enhanced approximately fourfold in the presence of ARL-67156 (Fig. 7A, bottom row). The AA of the right side of the cell-free lane in these different conditions (Fig. 7B) is significantly different from the one in control condition.

Role of P2Y Receptors on Ca^{2+} Release in MS and NB Cells

To study the role of P2Y in IC, and since P2Y receptors are known to be coupled to PLC, we used the PLC inhibitor U-73122 (10 μM)[46] and its negative control U-73343 (10 μM). Pretreatment with U-73122 ($N = 19$) caused a reduction of the Ca^{2+} transient in the MS cell and an inhibition of the Ca^{2+} wave in the NB cells (only 50% of the NB1 cells showed a significant Ca^{2+} increase), whereas its negative control, U-73343, did not have any effect on the IC ($N = 26$; Fig. 8). These results suggest that PMS resulted in activation of PLC in the NB cells, and thus, that IP_3-induced Ca^{2+} release plays a role in the propagation of the intercellular Ca^{2+} wave.

DISCUSSION

Characteristic Ca^{2+} waves in cellular monolayers are a manifestation of IC. In nonexcitable cells, Ca^{2+} waves can be propagated by PIC and/or GJIC. This study has investigated, for the first time, intercellular Ca^{2+} wave propagation in corneal endothelial cells with a focus on characterization of a PIC pathway. Our major finding is that the propagation of a Ca^{2+} wave in response to PMS is sustained partially by ATP-mediated PIC. The extent of propagation of the Ca^{2+} wave is limited by the ectonucleotidases present on the plasma membrane that metabolize ATP.

Ca^{2+} Increase in MS Cells

BCECs responded to PMS by a $[Ca^{2+}]_i$ transient (Fig. 2A). Such a response has been recorded in several cell types, including vascular endothelium, astrocytes, osteoblasts, and a wide variety of epithelial cells.[26,27,29,30,47–51] The response is characterized by a rapid onset to a peak followed by slow decay toward the baseline. The Ca^{2+} transients evoked by PMS in our experiments result from mechanotransduction and are not due to damage of the plasma membrane. In the unusual cases of membrane damage, we noticed a precipitous loss of fluorescent label (Fluo-4; Molecular Probes) from the MS cell. Experiments with such rapid fluorescence losses were promptly discarded from further consideration. The mechanisms for the Ca^{2+} increase in the MS cell, although not examined in detail, could be attributed to Ca^{2+} influx through putative stretch-activated cation channels, release of Ca^{2+} from endoplasmic reticulum (ER) stores secondary to activation of phospholipases, or autocrine effects of ATP release in response to membrane stretch. The contribution of Ca^{2+} release via a pathway involving PLC and IP_3 is supported by the finding that exposure to U-73122 partially inhibited the Ca^{2+} increase in the MS cell (Fig. 8).

Contribution of PIC toward Ca^{2+} Wave Propagation

Analysis of the wave propagation in terms of NF and %RC in the layers surrounding the MS cell offered several striking findings. The most noteworthy aspect is that the wave propagation could also occur along pathways devoid of cell–cell contacts (Fig. 3). This is clear proof of the involvement of a paracrine

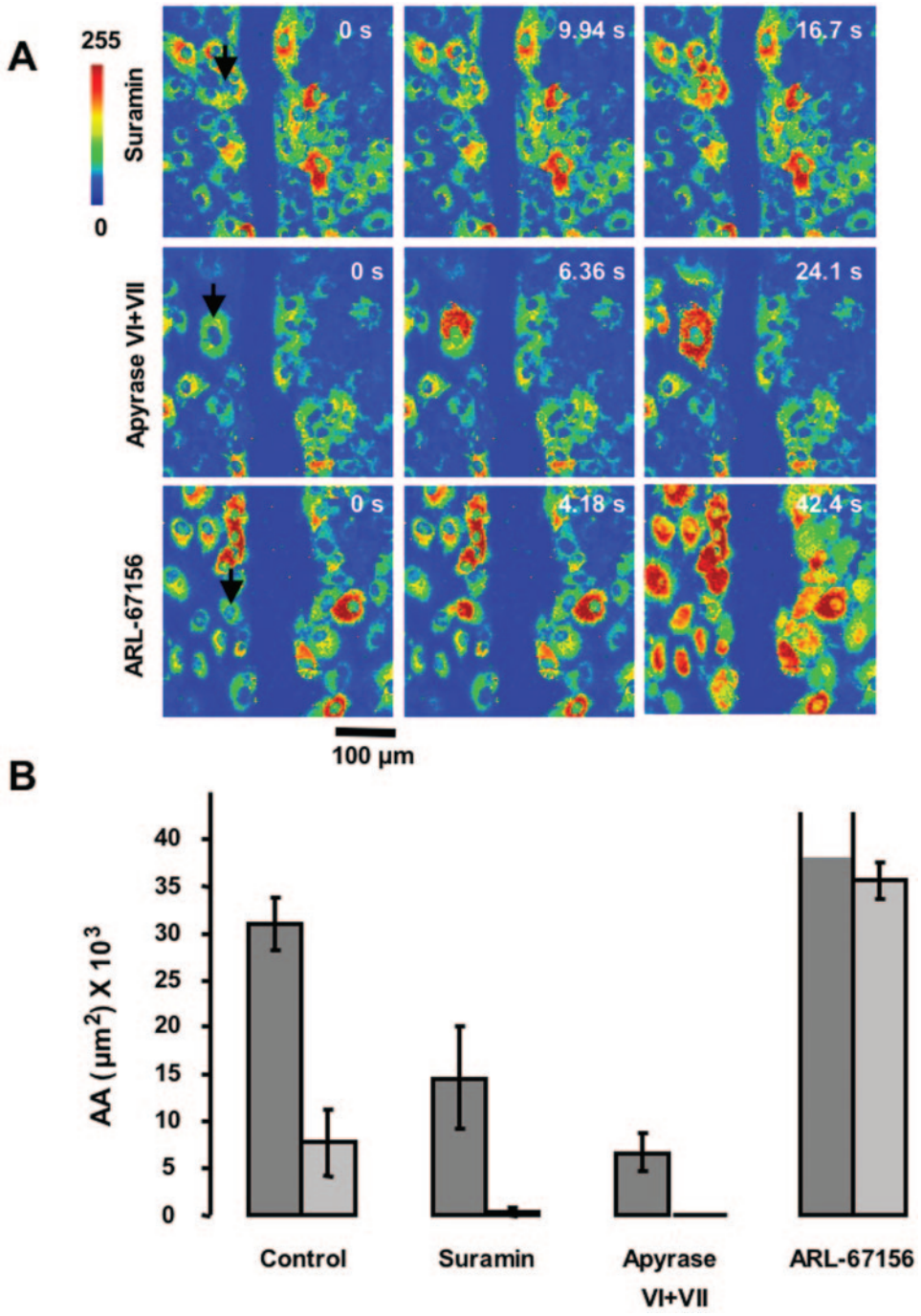

FIGURE 7. Effect of PIC inhibitors on Ca^{2+} wave propagation across cell-free lanes. (**A**) Fluorescence images of the Ca^{2+} wave in confluent cells with cell-free lanes. The different rows show the propagation in the presence of 200 μM suramin (N = 15; *top*), apyrase VI+VII (5 U/mL each; N = 13; *middle*), and 100 μM ARL-67156 (n = 16; *bottom*). *Arrow* in the first image of each row: MS cell. (**B**) AA of cells across the cell-free lane from five experiments of each of the different conditions. *Dark gray bars*: AA on the side of PMS; *light gray bars*: AA on the other side of the cell-free lane. *Dark gray open-ended bar* signifies that in the presence of ARL-67156 the AA on the side of the PMS exceeded the size of the image.

factor. In support of this claim, and further suggesting an involvement of P2Y receptors, we found that the propagated distance and the strength of the wave decreased significantly in the presence of suramin or U-73122 (Table 2, Fig. 8). This was further confirmed by receptor expression at the mRNA level, which indicated expression of P2Y1 and P2Y2 metabotropic receptors (Fig. 4B). In conjunction with these claims, the fact that the paracrine factor is ATP and/or its metabolites is made evident by the inhibitory effect of the exogenous apyrases on wave propagation. The finding that apyrase VII (which preferentially metabolizes ADP to AMP) was more potent than apyrase VI (which preferentially metabolizes ATP to ADP) is consistent with the fact that both ATP and ADP are agonists of P2Y1 and P2Y2 receptors. In fact, ADP is noted to be potent compared with ATP in activating the P2Y1 receptors.[21] AMP is not an agonist for either P2Y1 or P2Y2 receptors. The importance of ADP in PIC is emphasized in the enhanced inhibition of the wave propagation noted when cells were exposed to a combination of apyrase VI and apyrase VII (5 U/mL each).

Participation of GJIC in Ca^{2+} Wave Propagation

Although no direct conclusions can be drawn in favor of participation of GJIC in the observed wave propagation, it is important to note that U-73122, suramin, or apyrases did not completely inhibit the propagation. Srinivas et al.[37] have noted a complete inhibition of P2Y activity in cells pre-exposed to the PLC inhibitor U-73122. Moreover, connexin Cx43 has been shown to be present in BCECs, as demonstrated by immunocytochemistry.[52] Therefore, that there was not complete inhi-

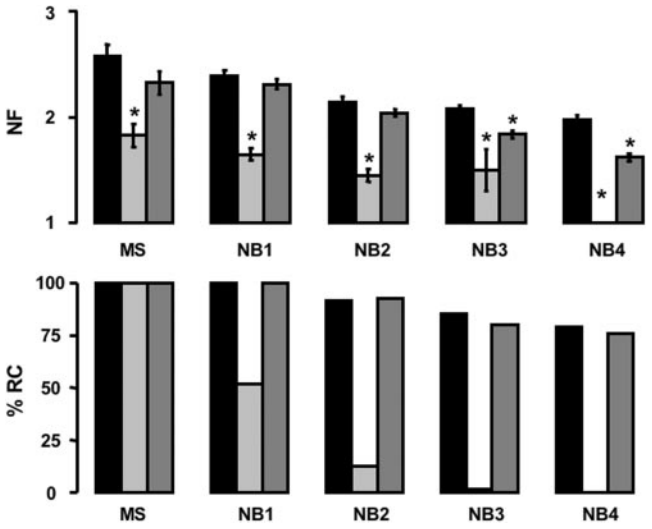

FIGURE 8. Ca^{2+} wave propagation in the presence of a PLC inhibitor. NF (*top*) and %RC (*bottom*) of BCECs in control conditions (*black bars*) or treated with U-73122 (10 μM; *light gray bars*) or with the inactive analogue U-73343 (10 μM; *dark gray bars*) for 30 minutes. $^{*}P < 0.05$ versus control.

bition of the wave is suggestive of GJIC superimposed on PIC, which is supported by the presence of Cx43 in BCECs.[52] This was consistent with the fact that neither suramin nor the exogenous apyrases affected the dye-coupling as noted in fluorescence recovery after photobleaching (FRAP) experiments in cells loaded with BCECF-AM (data not shown).

Role of Ectonucleotidases

Because in several cell types purinergic receptor activity is well known to be modulated by the activity of putative ectonucleotidases, we investigated their potential effect on PIC. Two prominent ectoenzymes that promote nucleotide metabolism are CD39 (ATP diphosphohydrolase, E.C. 3.6.1.5) and CD73 (5′-nucleotidase; E.C. 3.1.3.5).[53] CD39 is capable of ATP/ADP metabolism into AMP,[54,55] whereas CD73 degrades AMP to adenosine.[56,57] In BCECs, we found expression of both CD39 and CD73 at the mRNA level (Fig. 4B). Motivated by these findings, we investigated the effects of a putative, nonspecific ectonucleotidase inhibitor, ARL-67156, on Ca^{2+} wave propagation. The drug enhanced both the distance and the strength of the Ca^{2+} wave propagation. More specifically, ARL-67156 increased the AA of the Ca^{2+} wave threefold, enhanced the velocity of the propagation, and produced a three- to fourfold increase in Ca^{2+}-sensitive fluorescence integrated over the AA. Expression of CD73 is also important because adenosine, which is known to activate the A2B subtype of P1 receptors in corneal endothelium, would result in elevated cAMP and thereby may promote GJIC.[58,59]

Significance of PIC in Corneal Endothelium

As a form of IC, the importance of PIC to endothelial homeostasis cannot be underestimated, despite expression of connexins and functional GJIC, as evidenced by dye coupling.[60–62] In retinal pigmented epithelial cells (RPE cells), which express different isoforms of connexins, Ca^{2+} wave propagation is promoted by functional GJIC.[63,64] However, similar experiments with calf pulmonary artery endothelial (CPAE) cells indicated that expression of connexins and dye-coupling are not sufficient for Ca^{2+} wave propagation through gap junctions.[27] Furthermore, Ca^{2+} wave propagation in CPAE cells was unaffected by the putative GJIC blockers.[27] However, suramin and exogenous apyrases abolished the Ca^{2+} wave to a significant extent, indicating an involvement of purinergic receptors in Ca^{2+} wave propagation. Unlike P2X receptors, P2Y are coupled to $G_{\alpha q/11}$. The results of PIC in BCECs reported in this study are comparable to those found in CPAE cells, although the role of GJIC in Ca^{2+} wave propagation is yet to be fully examined.

In addition to the role of IC under resting conditions, it may be useful to speculate on the potential of our findings in the context of phacoemulsification. As shown in several studies, despite the use of viscoelastic agents, functional decompensation and loss of endothelial cells after phacoemulsification appear to be inevitable.[65–68] These effects are attributed to compressive stresses on the endothelium by the bursting of microbubbles induced by acoustic cavitation.[69,70] Each of these bursts causes a transient point source of stress similar to the PMS in this study. Therefore, it would be pertinent to examine further whether the probable IC induced during phaco-emulsification results in apoptosis in cells next to sites of local injury (akin to the bystander effect known to be mediated by gap junctions[71–73]) or promotes a tissue-wide defensive response to overcome the acute mechanical stress.

In conclusion, this study has delineated an important role for ATP in the corneal endothelium as a paracrine factor in cell–cell communication. Further investigation of the mechanism(s) of ATP release and putative roles of PIC would be helpful in understanding the pathophysiology of corneal endothelium.

References

1. Dikstein S, Maurice DM. The metabolic basis to the fluid pump in the cornea. *J Physiol*. 1972;221:29–41.
2. Bonanno JA. Identity and regulation of ion transport mechanisms in the corneal endothelium. *Prog Retin Eye Res*. 2003;22:69–94.
3. Fischbarg J, Hernandez J, Liebovitch LS, Koniarek JP. The mechanism of fluid and electrolyte transport across corneal endothelium: critical revision and update of a model. *Curr Eye Res*. 1985;4:351–360.
4. Riley M. Pump and leak in regulation of fluid transport in rabbit cornea. *Curr Eye Res*. 1985;4:371–376.
5. Candia OA. Electrolyte and fluid transport across corneal, conjunctival and lens epithelia. *Exp Eye Res*. 2004;78:527–535.
6. Walkenbach RJ, Chao WT. Adenosine regulation of cyclic AMP in corneal endothelium. *J Ocul Pharmacol*. 1985;1:337–342.
7. Walkenbach RJ, Ye GS, Reinach PS, Boney F. Alpha 1-adrenoceptors in the corneal endothelium. *Exp Eye Res*. 1992;55:443–450.
8. Jumblatt MM. Autocrine regulation of corneal endothelium by prostaglandin E2. *Invest Ophthalmol Vis Sci*. 1994;35:2783–2790.
9. Zhang Y, Xie Q, Sun XC, Bonanno JA. Enhancement of HCO_3^- permeability across the apical membrane of bovine corneal endothelium by multiple signaling pathways. *Invest Ophthalmol Vis Sci*. 2002;43:1146–1153.
10. Riley MV, Winkler BS, Starnes CA, Peters MI. Adenosine promotes regulation of corneal hydration through cyclic adenosine monophosphate. *Invest Ophthalmol Vis Sci*. 1996;37:1–10.
11. Riley MV, Winkler BS, Starnes CA, et al. Regulation of corneal endothelial barrier function by adenosine, cyclic AMP, and protein kinases. *Invest Ophthalmol Vis Sci*. 1998;39:2076–2084.
12. Wigham CG, Turner HC, Swan J, Hodson SA. Modulation of corneal endothelial hydration control mechanisms by Rolipram. *Pflugers Arch*. 2000;440:866–870.
13. Yasukura T, Inoue M, Irie T, et al. Adrenergic receptor-mediated Cl^- transport in rabbit corneal endothelial cells. *Jpn J Pharmacol*. 1995;67:315–320.
14. Srinivas SP, Yeh JC, Ong A, Bonanno JA. Ca^{2+} mobilization in bovine corneal endothelial cells by P2 purinergic receptors. *Curr Eye Res*. 1998;17:994–1004.
15. Cha SH, Hahn TW, Sekine T, et al. Purinoceptor-mediated calcium mobilization and cellular proliferation in cultured bovine corneal endothelial cells. *Jpn J Pharmacol*. 2000;82:181–187.

16. Leipziger J. Control of epithelial transport via luminal P2 receptors. *Am J Physiol*. 2003;284:F419–F432.
17. Jacobson KA, Jarvis MF, Williams M. Purine and pyrimidine (P2) receptors as drug targets. *J Med Chem*. 2002;45:4057–4093.
18. Inscho EW. P2 receptors in regulation of renal microvascular function. *Am J Physiol*. 2001;280:F927–F944.
19. Burnstock G, Williams M. P2 purinergic receptors: modulation of cell function and therapeutic potential. *J Pharmacol Exp Ther*. 2000;295:862–869.
20. Bailey MA, Hillman KA, Unwin RJ. P2 receptors in the kidney. *J Auton Nerv Syst*. 2000;81:264–270.
21. Ralevic V. P2 receptors in the central and peripheral nervous systems modulating sympathetic vasomotor tone. *J Auton Nerv Syst*. 2000;81:205–211.
22. Jacobson KA, Hoffmann C, Kim YC, et al. Molecular recognition in P2 receptors: ligand development aided by molecular modeling and mutagenesis. *Prog Brain Res*. 1999;120:119–132.
23. Apasov S, Koshiba M, Redegeld F, Sitkovsky MV. Role of extracellular ATP and P1 and P2 classes of purinergic receptors in T-cell development and cytotoxic T lymphocyte effector functions. *Immunol Rev*. 1995;146:5–19.
24. Harden TK, Boyer JL, Nicholas RA. P2-purinergic receptors: subtype-associated signaling responses and structure. *Annu Rev Pharmacol Toxicol*. 1995;35:541–579.
25. Anderson CM, Bergher JP, Swanson RA. ATP-induced ATP release from astrocytes. *J Neurochem*. 2004;88:246–256.
26. Newman EA. Propagation of intercellular calcium waves in retinal astrocytes and Muller cells. *J Neurosci*. 2001;21:2215–2223.
27. Moerenhout M, Himpens B, Vereecke J. Intercellular communication upon mechanical stimulation of CPAE-endothelial cells is mediated by nucleotides. *Cell Calcium*. 2001;29:125–136.
28. Cotrina ML, Lin JH, Lopez-Garcia JC, et al. ATP-mediated glia signaling. *J Neurosci*. 2000;20:2835–2844.
29. Homolya L, Steinberg TH, Boucher RC. Cell to cell communication in response to mechanical stress via bilateral release of ATP and UTP in polarized epithelia. *J Cell Biol*. 2000;150:1349–1360.
30. Evans JH, Sanderson MJ. Intracellular calcium oscillations induced by ATP in airway epithelial cells. *Am J Physiol*. 1999;277:L30–L41.
31. Osipchuk Y, Cahalan M. Cell-to-cell spread of calcium signals mediated by ATP receptors in mast cells. *Nature*. 1992;359:241–244.
32. Goodenough DA, Paul DL. Beyond the gap: functions of unpaired connexon channels. *Nat Rev Mol Cell Biol*. 2003;4:285–294.
33. Xie HQ, Hu VW. Modulation of gap junctions in senescent endothelial cells. *Exp Cell Res*. 1994;214:172–176.
34. Cotrina ML, Gao Q, Lin JH, Nedergaard M. Expression and function of astrocytic gap junctions in aging. *Brain Res*. 2001;901:55–61.
35. Zhao W, Lin ZX, Zhang ZQ. Cisplatin-induced premature senescence with concomitant reduction of gap junctions in human fibroblasts. *Cell Res*. 2004;14:60–66.
36. Del Monte U, Statuto M. Drop of connexins: a possible link between aging and cancer? *Exp Gerontol*. 2004;39:273–275.
37. Srinivas SP, Ong A, Goon L, Bonanno JA. Lysosomal Ca^{2+} stores in bovine corneal endothelium. *Invest Ophthalmol Vis Sci*. 2002;43:2341–2350.
38. MacCallum DK, Lillie JH, Scaletta LJ, et al. Bovine corneal endothelium in vitro: elaboration and organization and of a basement membrane. *Exp Cell Res*. 1982;139:1–13.
39. Jelamskii S, Sun XC, Herse P, Bonanno JA. Basolateral Na^+-K^+-$2Cl^-$ cotransport in cultured and fresh bovine corneal endothelium. *Invest Ophthalmol Vis Sci*. 2000;41:488–495.
40. Diecke FP, Wen Q, Sanchez JM, et al. Immunocytochemical localization of Na^+-HCO_3^- cotransporters and carbonic anhydrase dependence of fluid transport in corneal endothelial cells. *Am J Physiol*. 2004;286:C1434–C1442.
41. Sun XC, Bonanno JA, Jelamskii S, Xie Q. Expression and localization of Na^+-HCO_3^- cotransporter in bovine corneal endothelium. *Am J Physiol*. 2000;279:C1648–C1655.
42. Sun XC, McCutheon C, Bertram P, et al. Studies on the expression of mRNA for anion transport related proteins in corneal endothelial cells. *Curr Eye Res*. 2001;22:1–7.
43. Sun XC, Bonanno JA. Expression, localization, and functional evaluation of CFTR in bovine corneal endothelial cells. *Am J Physiol*. 2002;282:C673–C683.
44. Ralevic V, Burnstock G. Receptors for purines and pyrimidines. *Pharmacol Rev*. 1998;50:413–492.
45. Westfall TD, Menzies JR, Liberman R, et al. Release of a soluble ATPase from the rabbit isolated vas deferens during nerve stimulation. *Br J Pharmacol*. 2000;131:909–914.
46. Yule DI, Williams JA. U73122 inhibits Ca^{2+} oscillations in response to cholecystokinin and carbachol but not to JMV-180 in rat pancreatic acinar cells. *J Biol Chem*. 1992;267:13830–13835.
47. Churchill GC, Lurtz MM, Louis CF. Ca^{2+} regulation of gap junctional coupling in lens epithelial cells. *Am J Physiol*. 2001;281:C972–C981.
48. Shiga H, Tojima T, Ito E. Ca^{2+} signaling regulated by an ATP-dependent autocrine mechanism in astrocytes. *Neuroreport*. 2001;12:2619–2622.
49. Stout CE, Costantin JL, Naus CC, Charles AC. Intercellular calcium signaling in astrocytes via ATP release through connexin hemichannels. *J Biol Chem*. 2002;277:10482–10488.
50. Gomez P, Vereecke J, Himpens B. Intra- and intercellular Ca^{2+}-transient propagation in normal and high glucose solutions in ROS cells during mechanical stimulation. *Cell Calcium*. 2001;29:137–148.
51. Stalmans P, Himpens B. Confocal imaging of Ca^{2+} signaling in cultured rat retinal pigment epithelial cells during mechanical and pharmacologic stimulation. *Invest Ophthalmol Vis Sci*. 1997;38:176–187.
52. Mohay J, McLaughlin BJ. Corneal endothelial wound repair in normal and mitotically inhibited cultures. *Graefes Arch Clin Exp Ophthalmol*. 1995;233:727–736.
53. Farahbakhsh NA. Ectonucleotidases of the rabbit ciliary body nonpigmented epithelium. *Invest Ophthalmol Vis Sci*. 2003;44:3952–3960.
54. Marcus AJ, Broekman MJ, Drosopoulos JH, et al. Metabolic control of excessive extracellular nucleotide accumulation by CD39/ectonucleotidase-1: implications for ischemic vascular diseases. *J Pharmacol Exp Ther*. 2003;305:9–16.
55. Kittel A, Kaczmarek E, Sevigny J, et al. CD39 as a caveolar-associated ectonucleotidase. *Biochem Biophys Res Commun*. 1999;262:596–599.
56. Napieralski R, Kempkes B, Gutensohn W. Evidence for coordinated induction and repression of ecto-5′-nucleotidase (CD73) and the A2a adenosine receptor in a human B cell line. *Biol Chem*. 2003;384:483–487.
57. Hashikawa T, Takedachi M, Terakura M, et al. Involvement of CD73 (ecto-5′-nucleotidase) in adenosine generation by human gingival fibroblasts. *J Dent Res*. 2003;82:888–892.
58. Chanson M, White MM, Garber SS. cAMP promotes gap junctional coupling in T84 cells. *Am J Physiol*. 1996;271:C533–C549.
59. TenBroek EM, Lampe PD, Solan JL, et al. Ser364 of connexin43 and the upregulation of gap junction assembly by cAMP. *J Cell Biol*. 2001;155:1307–1318.
60. Watsky MA, Rae JL. Dye coupling in the corneal endothelium: effects of ouabain and extracellular calcium removal. *Cell Tissue Res*. 1992;269:57–63.
61. Williams K, Watsky M. Gap junctional communication in the human corneal endothelium and epithelium. *Curr Eye Res*. 2002;25:29–36.
62. Williams KK, Watsky MA. Bicarbonate promotes dye coupling in the epithelium and endothelium of the rabbit cornea. *Curr Eye Res*. 2004;28:109–120.
63. Stalmans P, Himpens B. Properties of intra- and intercellular Ca^{2+}-wave propagation elicited by mechanical stimulation in cultured RPE cells. *Cell Calcium*. 1999;25:391–399.
64. Himpens B, Stalmans P, Gomez P, et al. Intra- and intercellular Ca^{2+} signaling in retinal pigment epithelial cells during mechanical stimulation. *FASEB J*. 1999;13:S63–S68.
65. Bourne WM, McLaren JW. Clinical responses of the corneal endothelium. *Exp Eye Res*. 2004;78:561–572.

66. Bourne RR, Minassian DC, Dart JK, et al. Effect of cataract surgery on the corneal endothelium: modern phacoemulsification compared with extracapsular cataract surgery. *Ophthalmology*. 2004; 111:679–685.
67. Pirazzoli G, D'Eliseo D, Ziosi M, Acciarri R. Effects of phacoemulsification time on the corneal endothelium using phacofracture and phaco chop techniques. *J Cataract Refract Surg*. 1996;22:967–969.
68. Edelhauser HF. The resiliency of the corneal endothelium to refractive and intraocular surgery. *Cornea*. 2000;19:263–273.
69. Topaz M, Motiei M, Assia E, et al. Acoustic cavitation in phacoemulsification: chemical effects, modes of action and cavitation index. *Ultrasound Med Biol*. 2002;28:775–784.
70. Pacifico RL. Ultrasonic energy in phacoemulsification: mechanical cutting and cavitation. *J Cataract Refract Surg*. 1994;20:338–341.
71. Seymour C, Mothersill C. Cell communication and the "bystander effect". *Radiat Res*. 1999;151:505–506.
72. Wright EG. Commentary on radiation-induced bystander effects. *Hum Exp Toxicol*. 2004;23:91–94.
73. Edwards GO, Botchway SW, Hirst G, et al. Gap junction communication dynamics and bystander effects from ultrasoft X-rays. *Br J Cancer*. 2004;90:1450–1456.